Al-Rafidain Journal of Computer Sciences and Mathematics (RJCM)

www.csmj.mosuljournals.com

Numerical Solution for Fluid Flow in Horizontal and Inclined Cavities

Iman Hashim Al-obaidi

University of Mosul, College of Education for Pure Science, Iraq
Email: emanhashem1986@uomosul.edu.iq

Article information

Article history:
Received: 24/12/2023
Accepted :6/2/2024
Available online: 25/6/2024

Abstract

This study demonstrates how to control fluid flow in inclined and horizontal cavities. The equations governing the problem are established, including the two-dimensional nonlinear partial differential equations of energy, motion, and continuity. We use the successive implicit direction method (ADI) to numerically solve these equations. We discovered that the Rayleigh, Prandtl, Darcy, Eckert, and Reynolds numbers influenced the action of motion and energy equations, in addition to the effect of the problem's inclination angle. So, we solved this scheme by creating a computer program in MATLAB.

Keywords:
ADI method, Heat Transfer, Rayleigh number, Prandtl number, Darcy number.

Correspondence:
Author: **Iman Hashim Al-obaidi**
Email: *emanhashem1986@uomosul.edu.iq*

1. Introduction

Fluid is a substance that, in the absence of a poignant, cannot withstand stress or shear. Real, ideal, turbulent, laminar, constant, unstable, incompressible, compressible, uniform, and other flow behaviors can be classified [1]. Convection of MHD occurs through porous material at parallel surface boundaries as a result of precipitation and personal interactions in which it is involved [2]. The glass cavity stability analysis has been shortened by taking into account the structures that may or may not be identified by disturbance evolution after linear equations have been generated [3]. By smoothly injecting fluid from the opposite side of the channel into an upward tunnel with porous stockades, a fixed-state 3D MHD fluid flow can be analyzed to obtain heat transfer turfs and velocity analytical resolutions [4]. We investigated the velocity and thermal sliding of calculation remedies for a constant state MHD varied constrained boundaries sheet flow and heat transfer over an absorbent plate. It was discovered that the MF increases the velocity of a gelatinous inflexible fluid, lowering its temperature due to the stream's short-term drag [5]. We determined the regional Nusselt coefficients and friction with the skin factor, as well as non-Newtonian liquid inactive point flow and heat transfer across a stretching or shrinking slippage in a permeable center [6]. When thermal radiation is present, the 2D stable state hydromagnetic sticky fluid flow between two identical saucers with an increase in the variable suction limitation and the number of Reynolds and a relationship between the thermal extraction parameter, a decrease in temperature, and the concentration of the fluid was shown to exhibit an external transfer effect, a thick suction parameter, and a dissipative end result [7]. The effects of the equation on wave, heat transfer, and diffusion in a porous environment with radiation and MF attendance will be studied using a computerized solution[8].[9]discovered an instable MHD-free turbulent river over an oblique dish in a 2D direct system and used an explicit finite difference algorithm to investigate its equilibrium requirements.[10] revealed that a flexible framework involving steel sheets, heat argument flux, and a boiler allowed for the cyclical transfer of heat and flow in the region of oblique ferrites. [11] to properly solve a set of partial differential equations that describe the situation using linear proximity, investigate how fluid flow occurs in a bridge when electromagnetism (EMF) is present. Similarly, we want to show how tangible factors influence everything and how temperatures vary within the section. [12] investigated how thermal absorption and Dufour influenced the occasional free magnetism anatomy of heat transfer via an unrestricted vertical impervious surface.The outcome of this investigation will be given and truly conveyed in a movable parallel square layer for common features with parameter modifications to investigate quantitatively transient reciprocal mass and heat transfer via mixed air flow[13].The goal of this project is to examine the computerized solution to the fluid flow problem encountered in inclined and horizontal cavities using the ADI.We discovered that the constraints Da , $\mathcal{Re}$, $\mathcal{Pr}$, Ec , $\mathcal{Ra}$. and φ had a significant effect on the increase and decrease of the fluid inside the cavity, as well as the effect of time steps on this equation

2. Mathematical Model and Essential Equations

The two vertical heat-conducting walls in the mathematical model represent the inner layers of the two glass panels that comprise the glass chamber. These two walls are perpendicular to the $y-axis$ and have two horizontal heat-insulating walls perpendicular to the $x-axis$ One of the walls is hot, and its temperature is represented by the symbol T_1, while the other is cool, and its temperature is represented by the symbol T_0. The length of the connecting walls is L, and the length of the insulating walls is H . As shown in Figure 1, this cavity is filled with an incompressible fluid with a viscosity dispersion.

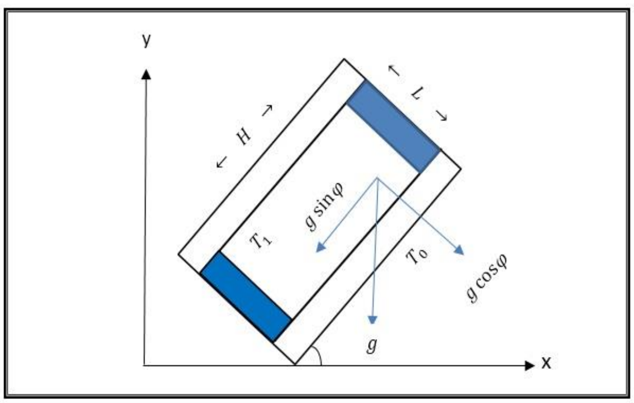

Fig. 1. Demonstrates a physical model and a coordinate system.

Below are the main governing equations, which also include the equations of Continuity, movement and energy:

$$\frac{\partial u}{\partial x}+\frac{\partial v}{\partial y}=0 \qquad (1)$$

$$\frac{\partial u}{\partial t}+u\frac{\partial u}{\partial x}+v\frac{\partial u}{\partial y} = -\frac{1}{\rho}\frac{\partial p}{\partial x}+\upsilon\nabla^2 u+\frac{v}{k}u - \beta g(T-T_0)\cos\varphi \qquad (2)$$

$$\frac{\partial v}{\partial t}+u\frac{\partial v}{\partial x}+v\frac{\partial v}{\partial y} = -\frac{1}{\rho}\frac{\partial p}{\partial y}+\upsilon\nabla^2 v + \beta g(T-T_0)\ \sin\varphi \qquad (3)$$

We may derive equations (2), (3) with regard to $x$and y, and then subtract the resulting equations to get-

$$\frac{\partial}{\partial t}\left[\frac{\partial v}{\partial x}-\frac{\partial u}{\partial y}\right]+\frac{\partial}{\partial x}\left[u\frac{\partial v}{\partial x}+v\frac{\partial v}{\partial y}\right]-\frac{\partial}{\partial y}\left[u\frac{\partial u}{\partial x}+v\frac{\partial u}{\partial y}\right]=$$

$$=\upsilon\nabla^2\left[\frac{\partial v}{\partial x}-\frac{\partial u}{\partial y}\right]-\frac{v}{k}\frac{\partial u}{\partial y}+\beta g\frac{\partial T}{\partial x}\ \sin\varphi + \beta g\frac{\partial T}{\partial y}\ \cos\varphi\ . \qquad (4)$$

This is known as the general of momentum equation.

The energy equation is:

$$\frac{\partial T}{\partial t}+u\frac{\partial T}{\partial x}+v\frac{\partial T}{\partial y}=\frac{k}{\rho C_p}\nabla^2 T+\varepsilon\left[\left(\frac{\partial u}{\partial y}\right)^2+\left(\frac{\partial v}{\partial x}\right)^2\right] \qquad (5)$$

Where $u, v$are the components of velocity in x, y directions respectively , t is the time and $\rho, v, \beta, g, T, k, C_p, \varepsilon$ are the density, kinematics viscosity, updraft expansion coefficient, gravitational acceleration, temperature, Permeability of medium , specific heat at constant pressure, The dispersion parameter, concentration respectively.

With the following boundary conditions,

$$\left.\begin{aligned} &T(0,y)=T_1\\ &T(L,y)=T_0\\ &\left.\frac{\partial T}{\partial y}\right|_{y=0,H}=0\\ &u(0,y)=v(0,y)=0\\ &u(L,y)=v(L,y)=0\\ &u(x,0)=v(x,0)=0\\ &u(x,H)=v(x,H)=0 \end{aligned}\right\} \qquad (6)$$

3. Dimensional Analysis

$$u^*=\frac{u}{U}\quad,\quad v^*=\frac{v}{U}\quad,\quad x^*=\frac{x}{L}\quad,\quad y^*=\frac{y}{L}$$

$$\left.\theta=\frac{T-T_0}{T_1-T_0}\quad,\quad t^*=\frac{tU}{L}\ ,\qquad p=p^*\rho U^2\right\}\quad(7)$$

And non- dimensional Parameters [16]:-

$$\left.\begin{aligned}
&U=\frac{\alpha}{L}\sqrt{RaPr}=\sqrt{g\beta\Delta TL}\\
&Ra=\frac{\rho g\beta(T_1-T_0)L^3}{\mu\alpha}\\
&Pr=\frac{\nu}{\alpha}=\frac{\mu C_p}{k}\quad,\qquad Da=\frac{k}{L^2}\\
&Ec=\frac{u^2}{C_p\Delta T}\\
&Re=\frac{LU}{\nu}\qquad,\qquad \varepsilon=\frac{\mu}{\rho C_p}
\end{aligned}\right\}\quad(8)$$

Where Ra Rayleigh Number, Pr Prandtel Number, Da Darcy Number, Re Reynolds Number and Ec Eckert Number.

By substituting non-dimensional values (7), into the equations (1), (4) and (5) we get:

$$\frac{\partial u^*}{\partial x^*}+\frac{\partial v^*}{\partial y^*}=0\qquad(9)$$

$$\frac{\partial}{\partial t^*}\left[\frac{\partial v^*}{\partial x^*}-\frac{\partial u^*}{\partial y^*}\right]+\frac{\partial}{\partial x^*}\left[u^*\frac{\partial v^*}{\partial x^*}+v^*\frac{\partial v^*}{\partial y^*}\right]-\frac{\partial}{\partial y^*}\left[u^*\frac{\partial u^*}{\partial x^*}+v^*\frac{\partial u^*}{\partial y^*}\right]=$$

$$\frac{1}{Re}\nabla^2\left[\frac{\partial v^*}{\partial x^*}-\frac{\partial u^*}{\partial y^*}\right]-Da^{-1}\sqrt{\frac{Pr}{Ra}}\frac{\partial u^*}{\partial y^*}+\frac{\alpha}{L}\sqrt{Ra\,Pr}\frac{\partial\theta}{\partial x^*}\ \sin\varphi$$

$$+\frac{\alpha}{L}\sqrt{Ra\,Pr}\frac{\partial\theta}{\partial y^*}\ \cos\varphi\ .\qquad(10)$$

But $u^*=\frac{\partial\psi}{\partial y^*}$ and $v^*=-\frac{\partial\psi}{\partial x^*}$ is stream function [17]. Put

$\xi=\nabla^2\psi$, then equation (10) become:

For the purpose of finding non-dimensional equations of equations (1), (4), (5) We will impose some non-dimensional values [14, 15]: -

$$\frac{\partial\xi}{\partial t^*}=\frac{1}{Re}\nabla^2\xi+Da^{-1}\sqrt{\frac{Pr}{Ra}}\frac{\partial^2\psi}{\partial {y^*}^2}-\frac{\alpha}{L}\sqrt{Ra\,Pr}\left[\frac{\partial\theta}{\partial x^*}\ \sin\varphi+\frac{\partial\theta}{\partial y^*}\ \cos\varphi\right]\qquad(11)$$

$$\frac{\partial\theta}{\partial t^*}+u^*\frac{\partial\theta}{\partial x^*}+v^*\frac{\partial\theta}{\partial y^*}=\frac{1}{\sqrt{Ra\,Pr}}\left[\frac{\partial^2\theta}{\partial {x^*}^2}+\frac{\partial^2\theta}{\partial {y^*}^2}\right]+\frac{Pr\,Ec}{\sqrt{Ra\,Pr}}\left[\left(\frac{\partial u^*}{\partial y^*}\right)^2+\left(\frac{\partial v^*}{\partial x^*}\right)^2\right]\qquad(12)$$

Let $\emptyset=\frac{Pr\,Ec}{\sqrt{Ra\,Pr}}\left[\left(\frac{\partial u^*}{\partial y^*}\right)^2+\left(\frac{\partial v^*}{\partial x^*}\right)^2\right]$ Physical quantities, and equation (12) becomes-

$$\frac{\partial\theta}{\partial t^*}+u^*\frac{\partial\theta}{\partial x^*}+v^*\frac{\partial\theta}{\partial y^*}=\frac{1}{\sqrt{Ra\,Pr}}\left[\frac{\partial^2\theta}{\partial x^*}+\frac{\partial^2\theta}{\partial y^*}\right]+\emptyset\qquad(13)$$

The resulting boundary conditions are:

$$\left.\begin{aligned}
&u^*=v^*=0\\
&\theta(0,y^*)=1\\
&\theta(L,y^*)=0\\
&\left.\frac{\partial\theta}{\partial y^*}\right|_{y^*=0,H}=0\\
&u(0,y^*)=v(0,y^*)=0\\
&u(L,y^*)=v(L,y^*)=0\\
&u(x^*,0)=v(x^*,0)=0\\
&u(x^*,H)=v(x^*,H)=0
\end{aligned}\right\}\quad(14)$$

4. Method of Solution

Starting with the last equation (13), the heat equation, and working our way down to equation (11), the motion equation, we can resolve the network of formulas (9), (11) and (13) with the boundary conditions (14) using the ADI finite difference technique [18].

4.1 Solving of the Heat Equation

$$\frac{\theta^*_{i,j}-\theta_{i,j,n}}{\frac{\Delta\tau^*}{2}}+u^*_{i.j.n}\frac{\theta^*_{i+1,j}-\theta^*_{i-1,j}}{2\Delta x^*}+v^*_{i.j.n}\frac{\theta_{i,j+1,n}-\theta_{i,j-1,n}}{2\Delta y^*}=\frac{1}{\sqrt{Ra\,Pa}}\left[\frac{\theta^*_{i+1,j}-2\theta^*_{i,j}+\theta^*_{i-1,j}}{(\Delta x^*)^2}+\frac{\theta_{i,j+1,n}-2\theta_{i,j,n}+\theta_{i,j-1,n}}{(\Delta y^*)^2}\right]+\emptyset \qquad (15)$$

$$\frac{\theta_{i,j,n+1}-\theta^*_{i,j}}{\frac{\Delta\tau^*}{2}}+u^*_{i.j.n}\frac{\theta^*_{i+1,j}-\theta^*_{i-1,j}}{2\Delta x^*}+v^*_{i.j.n}\frac{\theta_{i,j+1,n+1}-\theta_{i,j-1,n+1}}{2\Delta y^*}=\frac{1}{\sqrt{Ra\,Pa}}\left[\frac{\theta^*_{i+1,j}-2\theta^*_{i,j}+\theta^*_{i-1,j}}{(\Delta x^*)^2}+\frac{\theta_{i,j+1,n+1}-2\theta_{i,j,n+1}+\theta_{i,j-1,n+1}}{(\Delta y^*)^2}\right]+\emptyset \qquad (16)$$

Equations (15) and (16) can be combined to yield,

$$A1_i\theta^*_{i-1,j}+B1_i\theta^*_{i,j}+C1_i\theta^*_{i+1,j}=D1_i \qquad i=0,1,2,3,\ldots\ldots N \qquad (17)$$

Where

$$A1_i=-1$$

$$B1_i=\frac{2f_1}{f_6}$$

$$C1_i=\frac{-f_2}{f_6}$$

$$D1_i=\frac{-f_3}{f_6}\theta_{i,j-1,n}+\frac{2f_4}{f_6}\theta_{i,j,n}+\frac{f_5}{f_6}\theta_{i,j+1,n}+\frac{\emptyset h^{*^2}}{f_6}$$

Followed by

$$A2_i\theta_{i,j-1,n+1}+B2_i\theta_{i,j,n+1}+C2_i\theta_{i,j+1,n+1}=D2_i \qquad (18)$$

Where,

$$A2_i=-1$$

$$B2_i=\frac{2f_1}{f_3}$$

$$C2_i=\frac{-f_5}{f_3}$$

$$D2_i=\frac{f_6}{f_3}\theta^*_{i-1,j}+\frac{2f_4}{f_3}\theta^*_{i,j}+\frac{f_2}{f_3}\theta^*_{i+1,j}+\frac{\emptyset h^{*^2}}{f_3}$$

Where,

$$=\left[\frac{1}{\lambda}+\frac{1}{\sqrt{RaPr}}\right], \qquad f_2=\left[\frac{1}{\sqrt{RaPr}}-\frac{h^*}{2}u^*_{i,j,n}\right]$$

$$f_3=\left[\frac{1}{\sqrt{RaPr}}+\frac{h^*}{2}v^*_{i,j,n}\right], \qquad f_4=\left[\frac{1}{\lambda}-\frac{1}{\sqrt{RaPr}}\right]$$

$$f_5=\left[\frac{1}{\sqrt{RaPr}}-\frac{h^*}{2}v^*_{i,j,n}\right], \quad f_6=\left[\frac{1}{\sqrt{RaPr}}+\frac{h^*}{2}u^*_{i,j,n}\right]$$

4.2 Solving of the General Motion Equation

$$\frac{\xi^*_{i,j}-\xi_{i,j,n}}{\frac{\Delta\tau^*}{2}}=\frac{1}{Re}\left[\frac{\xi^*_{i+1,j}-2\xi^*_{i,j}+\xi^*_{i-1,j}}{(\Delta x^*)^2}+\frac{\xi_{i.j+1,n}-2\xi_{i.j,n}+\xi_{i.j-1,n}}{(\Delta y^*)^2}\right]+Da^{-1}\sqrt{\frac{Pr}{Ra}}\left[\frac{\psi_{i,j+1,n}-2\psi_{i,j,n}+\psi_{i,j-1,n}}{(\Delta y^*)^2}\right]+\frac{\alpha}{L}\sqrt{RaPr}\left[\frac{\theta^*_{i+1,j}-\theta^*_{i-1,j}}{2\Delta x^*}\sin\varphi+\frac{\theta_{i,j+1,n}-\theta_{i,j-1,n}}{2\Delta y^*}\cos\varphi\right] \qquad (19)$$

$$\frac{\xi_{i,j,n+1}-\xi^*_{i,j}}{\frac{\Delta\tau^*}{2}}=\frac{1}{Re}\left[\frac{\xi^*_{i+1,j}-2\xi^*_{i,j}+\xi^*_{i-1,j}}{(\Delta x^*)^2}+\frac{\xi_{i.j+1,n+1}-2\xi_{i.j,n+1}+\xi_{i.j-1,n+1}}{(\Delta y^*)^2}\right]+Da^{-1}\sqrt{\frac{Pr}{Ra}}\left[\frac{\psi_{i,j+1,n+1}-2\psi_{i,j,n+1}+\psi_{i,j-1,n+1}}{(\Delta y^*)^2}\right]+\frac{\alpha}{L}\sqrt{RaPr}\left[\frac{\theta^*_{i+1,j}-\theta^*_{i-1,j}}{2\Delta x^*}\sin\varphi+\frac{\theta_{i,j+1,n+1}-\theta_{i,j-1,n+1}}{2\Delta y^*}\cos\varphi\right] \qquad (20)$$

Equations (19) and (20) can be reduced to give:

$$A3_i\xi^*_{i-1,j}+B3_i\xi^*_{i,j}+C3_i\xi^*_{i+1,j}=D3_i \qquad i=0,1,2,3,\ldots.N \qquad (21)$$

Where,

$A3_i = -1$

$B3_i = \frac{f_1}{f_2}$

$C3_i = -1$

$$D3_i = \xi_{i,j-1,n} + \left(\frac{f_3}{f_2}\right)\xi_{i,j,n} + \xi_{i,j+1,n} + \frac{\lambda}{2}Da^{-1}\sqrt{\frac{Pr}{Ra}}\left[\psi_{i,j+1,n} - 2\psi_{i,j,n} + \psi_{i,j-1,n}\right] + \frac{\alpha\lambda h^*}{4L}\sqrt{RaPr}\left[(\theta^*_{i+1,j} - \theta^*_{i-1,j})\sin\varphi + (\theta_{i,j+1,n} - \theta_{i,j-1,n})\cos\varphi\right]$$

Followed by

$$A4_i\xi_{i,j-1,n+1} + B4_i\xi_{i,j,n+1} + C4_i\xi_{i,j+1,n+1} = D4_i \qquad (22)$$

Where,

$A4_i = -1$

$B4_i = \frac{f_1}{f_2}$

$C4_i = -1$

$$D4_i = \xi^*_{i-1,j} + \frac{f_3}{f_2}\xi^*_{i,j} + \xi^*_{i+1,j} + \frac{\lambda}{2}Da^{-1}\sqrt{\frac{Pr}{Ra}}\left[\psi_{i,j+1,n+1} - 2\psi_{i,j,n+1} + \psi_{i,j-1,n+1}\right] + \frac{\alpha\lambda h^*}{4L}\sqrt{RaPr}\left[(\theta^*_{i+1,j} - \theta^*_{i-1,j})\sin\varphi + (\theta_{i,j+1,n} - \theta_{i,j-1,n+1})\cos\varphi\right]$$

Where,

$$f_1 = 1 + \frac{\lambda}{Re} \quad , \quad f_2 = \frac{\lambda}{2Re} \quad , \quad f_3 = 1 - \frac{\lambda}{Re}$$

The coefficients u^* and $v^*$are considered constants in the computation for each time step [19]. There is a three-diagonal form produced by both equations (motion and heat). Using the Gaussian elimination procedure, every element is given in [20].

5. Conclusion

The ADI method, which we used to solve the governing equations completely without decreasing or changing, is the most significant accomplishment of this work. Based on the results, we conclude that all equations can be solved to a stable state after a number of iterations, and at different angles 0, 30, and 90, the ADI method, as shown in the figures, is the most important achievement.

1. Increases the time step in the energy equation, causes a shift away from stability, as shown in **Fig. 2** and **Fig. 3**.
2. **Fig. 4** and **Fig. 7** show that as the Prandtl number in the energy and motion equation decreases, we get closer to stability at various points in time.
3. As shown in **Fig. 5** and **Fig. 8**, increasing the Rayleigh number in motion and energy equations accelerates reaching stability.
4. In energy equation, the more the Eckert number, the further we move away from stability as **Fig. 6**.
5. In the equation of motion, the greater angle, the further away we are from stability at the same point in time as in **Fig. 9**.
6. As the angle of inclination and the Prandtl number decrease, achieving stability accelerates as shown in **Fig. 10**.
7. In the equation of motion, we notice that increasing the Reynold, Rayleigh numbers and inclination angle leads to a move away from stability as shown in **Fig. 11** and **Fig. 12**.

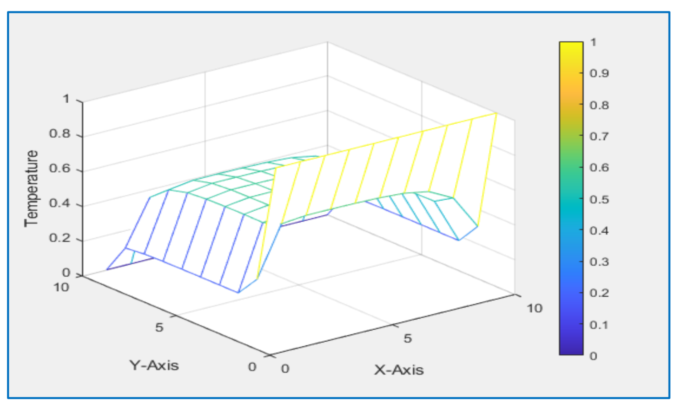

Fig. 2. Temperature behavior inside the channel.

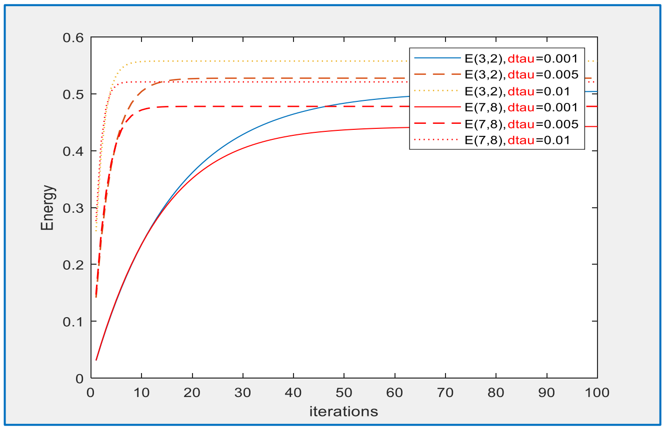

Fig. 3. Variation of temperature profile when **dtau**= (**0.001, 0.005, 0.01**).

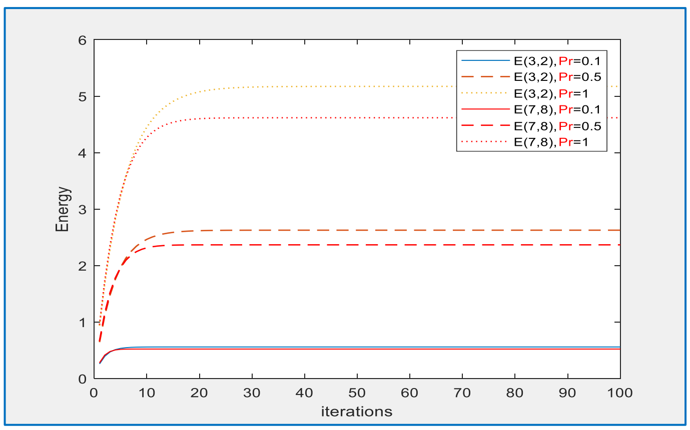

Fig. 4. Temperature profile variation for different value of $\boldsymbol{Pr} = (\mathbf{0.1}, \mathbf{0.5}, \mathbf{1})$.

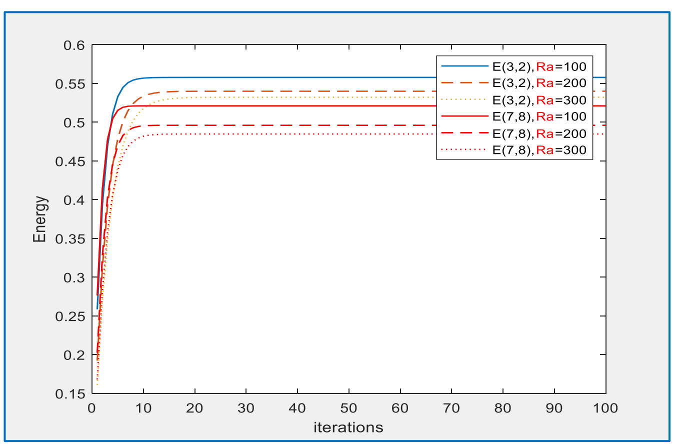

Fig. 5. Temperature Variance for different value of $\boldsymbol{Ra} = (\mathbf{100}, \mathbf{200}, \mathbf{300})$.

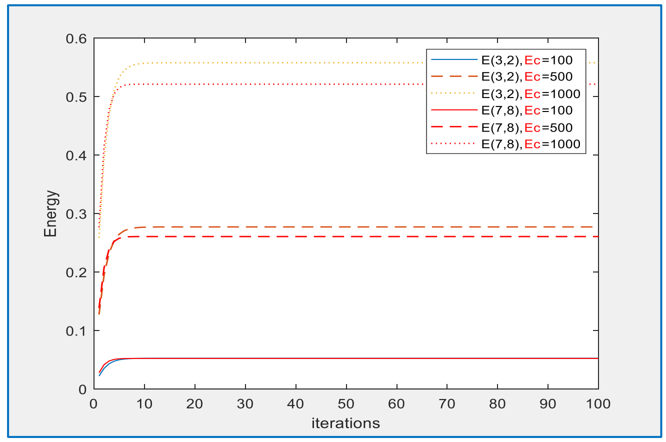

Fig. 6. Temperature variance for different value of $\boldsymbol{Ec} = (\mathbf{100}, \mathbf{500}, \mathbf{1000})$.

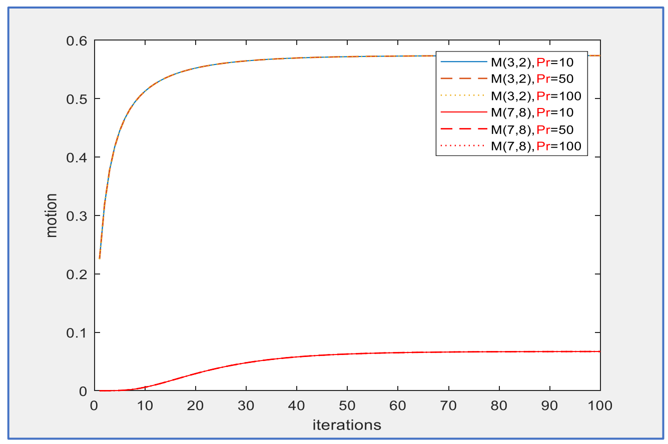

Fig. 7. Distinction of speed shape for several values of $\boldsymbol{Pr} = (\mathbf{10}, \mathbf{50}, \mathbf{100})$

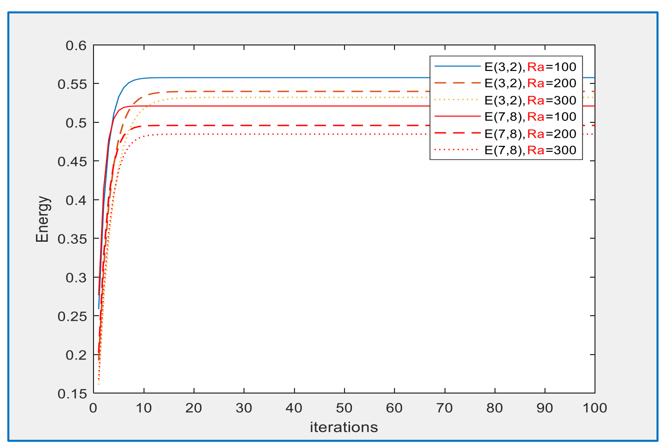

Fig. 8. change of velocity distribution for distinct $\boldsymbol{Ra} = (\mathbf{100}, \mathbf{500}, \mathbf{1000})$

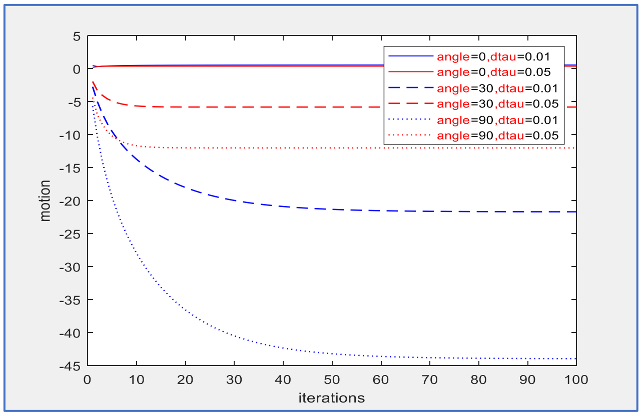

Fig. 9. Impact of duta-step on the motion equation at angles (0, 30, 90).

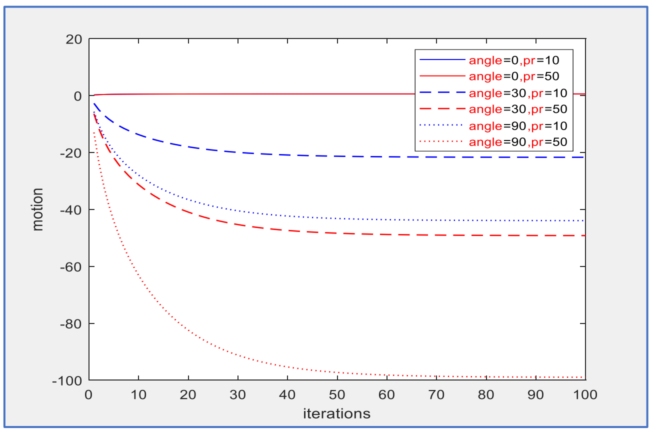

Fig. 10. Effect of Prandtel Number Pr on motion equation at angles (0, 30, 90).

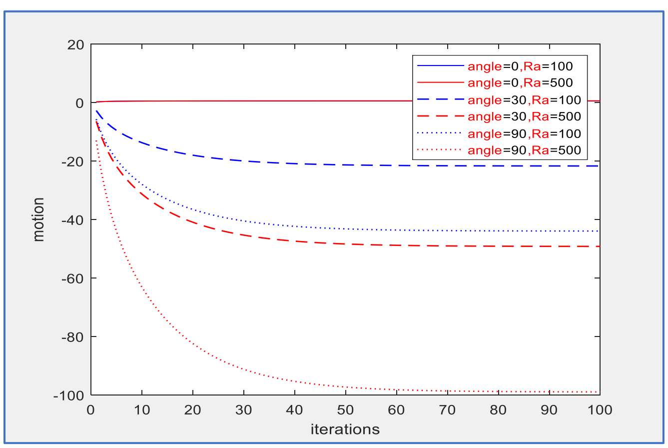

Fig. 11. Effect of Rayleigh Number Ra on motion equation at angles (0, 30, 90).

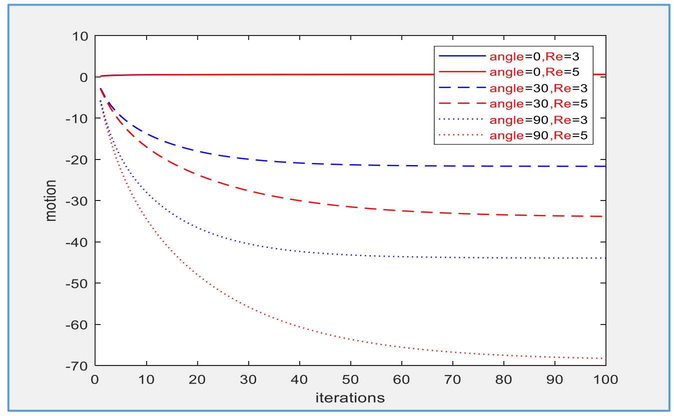

Fig. 12. Effect of Reynolds number Re on motion equation at angles (0, 30, 90)

References

[1] W. F. Hughes and J. A. Brighton, "Schaum's outline of theory and problems of fluid dynamics," *(No Title)*, 1967.

[2] G. S. Reddy, G. V. R. Reddy, and K. J. Reddy, "Radiation and chemical reaction effects on free convection MHD flow through a porous medium bounded by vertical surface," Adv. Appl. Sci. Res., vol. 3, no. 3, pp. 1603–1610, 2012.

[3] A. Hammodat and T. Shuker, "Stability Analysis of a Fluid in Horizontal and Oblique Glass Cavities," AL-Rafidain J. Comput. Sci. Math., vol. 11, pp. 89–97, 2014.

[4] K. Jabr, "Influence of MHD on Steady State Newtonian Fluid Flow in a Vertical Channel with Porous Wall using HAM," Iraqi J. Sci., vol. 55, no. 2B, pp. 811–821, 2014.

[5] S. Mukhopadhyay and I. C. Mandal, "Magnetohydrodynamic (MHD) mixed convection slip flow and heat transfer over a vertical porous plate," Eng. Sci. Technol. an Int. J., vol. 18, no. 1, pp. 98–105, 2015.

[6] A. Hammodat and A. I. Basheer, "MHD Stagnation-Point Flow of Non-Newtonian Fluid and Heat Transfer over Stretching/Shrinking Sheet in a Porous Medium," J. Educ. Sci., vol. 28, no. 1, pp. 71–82, 2019.

[7] K. Kumari and M. Goyal, "Heat and mass transfer flow of MHD viscous dissipative fluid in a channel with a stretching and porous plate," *An Int. J. Appl. Math. Inf. Sci. Lett.*, vol. 5, no. 3, pp. 81–87, 2017.

[8] Z. A. Almishlih, "Numerical solution of fluid flow in horizontal tube under effects of radiation field," *Open Access Libr. J.*, vol. 7, no. 05, p. 1, 2020.

[9] M. S. Ullah, A. Tarammim, and M. J. Uddin, "A study of two dimensional unsteady MHD free convection flow over a vertical plate in the presence of radiation," *Open J. Fluid Dyn.*, vol. 11, no. 1, pp. 20–33, 2021.

[10] T. Mehta, R. Mehta, and A. Mehta, "Oscillatory fluid flow and heat transfer through porous medium between parallel plates with inclined magnetic field, radiative heat flux and heat source," Int. J. Appl. Mech. Eng., vol. 25, no. 2, 2020.

[11] A. Hammodat, G. Algwauish, and I. Al-Obaidi, "The Effects of Electrical Conductivity on Fluid Flow between Two Parallel Plates in a Porous Medioum," Iraqi J. Sci., pp. 4953–4963, 2021.

[12] M. Hasanuzzaman, M. Azad, A. Kalam, and M. Hossain, "Effects of Dufour and thermal diffusion on unsteady MHD free convection and mass transfer flow through an infinite vertical permeable sheet," SN Appl. Sci., vol. 3, no. 12, pp. 1–11, 2021.

[13] G. M. Algwauish, A. A. Hammodat, and H. D. Saleem, "A Numerical Simulation of Convection and Conduction Heat

Transfer for a Fluid in a Porous Medium," Eur. J. Pure Appl. Math., vol. 16, no. 2, pp. 833–846, 2023.

[14] C. Cookey and V. Omubo-Pepple, "On steady hydro genetic flow of a radiating viscous fluid through a horizontal channel in a porous media," AMARECAN J. Sci. Ind. Res. ISSN, pp. 203–208, 2010.

[15] D. Cimpean and I. Pop, "A study of entropy generation minimization in an inclined channel," WSEAS Trans Heat Mass Transf., vol. 6, no. 2, pp. 31–40, 2011.

[16] J. D. Logan, Applied mathematics. John Wiley & Sons, 2013.

[17] D. Halpern, H. B. Wilson, and L. H. Turcotte, Advanced mathematics and mechanics applications using MATLAB. CRC press, 2002.

[18] U. Ali, F. A. Abdullah, and S. T. Mohyud-Din, "Modified implicit fractional difference scheme for 2D modified anomalous fractional sub-diffusion equation," Adv. Differ. Equations, vol. 2017, no. 1, pp. 1–14, 2017.

[19] B. Carnahan, H. A. Luther, and J. O. Wilkes, "Applied numerical methods," (No Title), 1969.

[20] V. M. Soundalgekar, B. S. Jaiswal, A. G. Uplekar, and H. S. Takhar, "Transient free convection flow of viscous dissipative fluid past a semi-infinite vertical plate," Appl. Mech. Eng., vol. 4, no. 2, pp. 203–218, 1999.